



Identification of substituted 2-thio-6-oxo-1,6-dihydropyrimidines as inhibitors of human lactate dehydrogenase



Peter S. Dragovich^{a,*}, Benjamin P. Fauber^a, Laura B. Corson^a, Charles Z. Ding^b, Charles Eigenbrot^a, HongXiu Ge^b, Anthony M. Giannetti^a, Thomas Hunsaker^a, Sharada Labadie^a, Yichin Liu^a, Shiva Malek^a, Borlan Pan^a, David Peterson^a, Keith Pitts^a, Hans E. Purkey^a, Steve Sideris^a, Mark Ultsch^a, Erica VanderPorten^a, BinQing Wei^a, Qing Xu^b, Ivana Yen^a, Qin Yue^a, Huihui Zhang^b, Xuying Zhang^b

^a Genentech, Inc., 1 DNA Way, South San Francisco, CA 94080, USA

^b WuXi AppTec Co., Ltd, 288 Fute Zhong Road, Waigaoqiao Free Trade Zone, Shanghai 200131, PR China

ARTICLE INFO

Article history:

Received 16 March 2013

Revised 28 March 2013

Accepted 1 April 2013

Available online 10 April 2013

Keywords:

Lactate dehydrogenase

X-ray crystal structure

Glycolysis

Tumor metabolism

ABSTRACT

A novel 2-thio-6-oxo-1,6-dihydropyrimidine-containing inhibitor of human lactate dehydrogenase (LDH) was identified by high-throughput screening ($IC_{50} = 8.1 \mu\text{M}$). Biochemical, surface plasmon resonance, and saturation transfer difference NMR experiments indicated that the compound specifically associated with human LDHA in a manner that required simultaneous binding of the NADH co-factor. Structural variation of the screening hit resulted in significant improvements in LDHA biochemical inhibition activity (best $IC_{50} = 0.48 \mu\text{M}$). A crystal structure of an optimized compound bound to human LDHA was obtained and explained many of the observed structure–activity relationships.

© 2013 Elsevier Ltd. All rights reserved.

It has been known since the early 1900s that many tumors exhibit altered metabolic characteristics relative to normal, non-transformed tissues.¹ One example of such altered metabolism is related to the utilization of glucose. Many tumors increase the rate of glucose uptake relative to normal cells and metabolize this nutrient primarily via glycolysis as opposed to the more energy-efficient but oxygen-dependent mitochondrial oxidative phosphorylation process.² In contrast to normal tissues which typically employ glycolysis only when oxygen supplies limit oxidative phosphorylation (e.g., strenuously working muscle), such glycolytic glucose consumption occurs in cancer cells even in the presence of abundant oxygen levels.² Originally described by Warburg,³ ‘aerobic glycolysis’ is currently viewed as an attractive differentiator between tumors and healthy tissues that can potentially be exploited for the development of new anti-cancer agents.⁴

Lactate dehydrogenase A (LDHA; also known as LDH-M and LDH-5) is a homotetrameric enzyme that catalyzes the cytosolic conversion of pyruvate to lactate in the final step of glycolysis (Fig. 1).^{5–7} This process involves a stereospecific hydride transfer from the reduced form of the associated nicotinamide adenine dinucleotide co-factor (NADH) to the pyruvate ketone moiety. An alternate lactate dehydrogenase isoform (LDHB; also known as

LDH-H and LDH-1) can also effect this transformation although it preferentially catalyzes the reverse reaction in which lactate is converted to pyruvate.^{5,7} LDHA is a HIF1 α and Myc target gene induced by hypoxia or mutations in VHL, FH, SDH, or the RAS/PI3K/AKT signaling pathways, and elevated LDHA levels are prevalent and associated with poor survival in many cancer indications.⁸ These observations suggest that LDHA may be an important contributor to the metabolic alterations required for the growth and proliferation of certain tumors. Indeed, shRNA-mediated LDHA knockdown in glycolytic cancer cell lines results in significant inhibition of tumor growth.⁹ Consistent with the function of LDHA in glycolysis, this growth reduction is more pronounced under hypoxic conditions where cells rely primarily on glycolytic energy production for survival.^{9a,c} Similarly, an LDHA inhibitor (**1**; FX-11, Fig. 2) exhibited *in vivo* activity against glycolytically dependent tumor xenograft models,¹⁰ although specific inhibition of the LDHA enzyme by this compound was not confirmed in recent experiments by others.¹¹ Importantly, humans who lack LDHA through hereditary deficiency display mild phenotypes suggesting that inhibition of the enzyme will not lead to significant intolerable side-effects.¹² Collectively, these data make LDHA an attractive target for the development of new anti-cancer agents for use against hypoxic and/or highly glycolytic tumors.

Several examples of human LDHA inhibitors previously reported in the literature are depicted in Figure 2.^{10,11,13,14} Some of

* Corresponding author. Tel.: +1 650 467 6854.

E-mail address: dragovich.peter@gene.com (P.S. Dragovich).

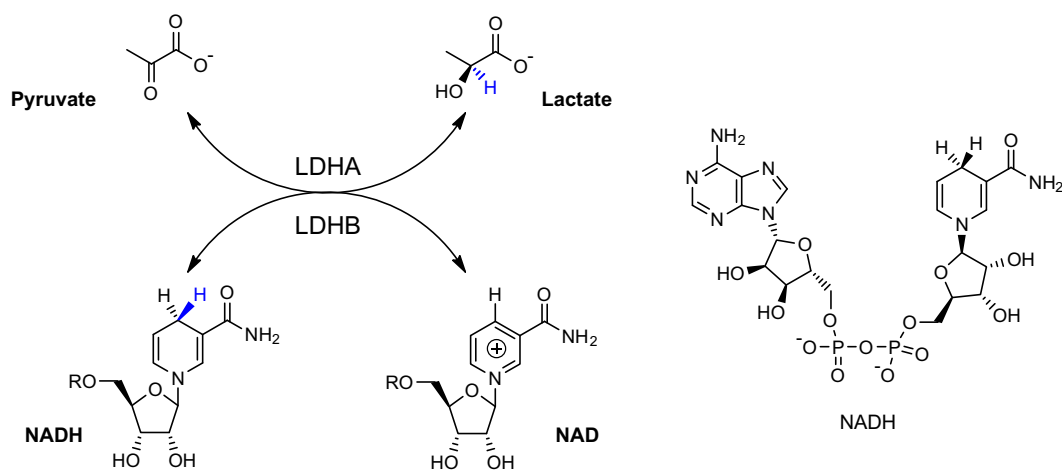


Figure 1. LDH biochemistry.

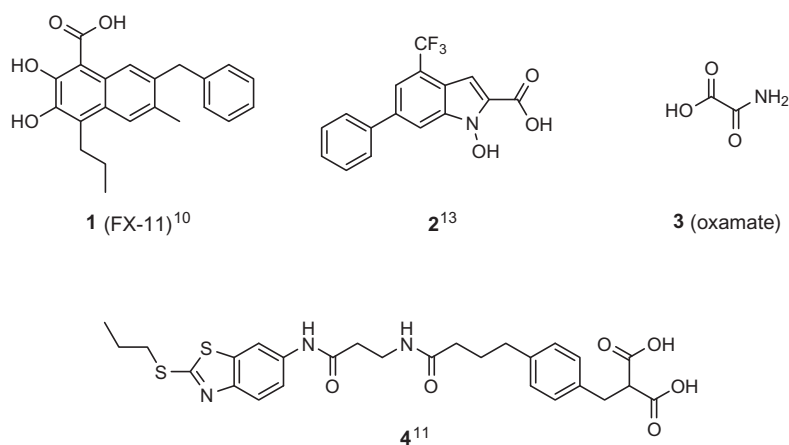
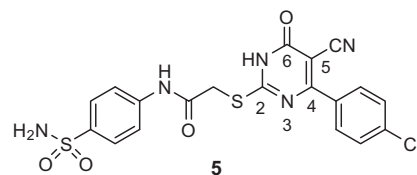


Figure 2. Structures of representative human LDHA inhibitors.

these molecules (e.g., compounds **1** and **2**) were recently described to exhibit ambiguous and/or weak LDHA associations¹¹ suggesting that the enzyme's biochemical activity may be susceptible to non-specific inhibition effects. Our own efforts to identify LDHA inhibitors began with high-throughput screening of the Roche and Genentech compound collections using a biochemical assay which spectrophotometrically monitored the disappearance of the NADH co-factor during enzymatic conversion of pyruvate to lactate.^{15,16} This screening identified a 2-thio-6-oxo-1,6-dihydropyrimidine¹⁷ as a moderately potent LDHA inhibitor (compound **5**, $IC_{50} = 8.8 \mu M$; Table 1). Importantly, a similar IC_{50} value was observed for the molecule when LDHA biochemical inhibition was quantitated via mass spectrometry, suggesting that the observed effects did not result from spectrophotometric artifacts (Table 1).¹⁶ In addition, biophysical surface plasmon resonance (SPR; Biacore) experiments conducted in the presence of NADH determined that the compound specifically associated with LDHA with a K_D that closely matched the biochemical IC_{50} value (Fig. 3A, Table 1).¹⁶ These results collectively suggested that compound **5** was a bona fide LDHA inhibitor worthy of further characterization.

Accordingly, additional biophysical experiments were conducted with **5** to better elucidate its LDHA inhibition mechanism. SPR assessments performed in the absence of NADH determined that the compound associated much more weakly with LDHA as compared with binding experiments conducted in the presence of the co-factor (compare Fig. 3A and B, Table 1). These results

Table 1
Structure and biological properties of compound **5**



Assay description ^a	Result (μM)
LDHA IC_{50} (UV endpoint)	8.8
LDHA IC_{50} (MS endpoint)	1.9
LDHA K_D (SPR, +NADH)	6.1
LDHA K_D (SPR, -NADH)	384
LDHB IC_{50} (UV endpoint)	11.1
MDH-1 IC_{50} (UV endpoint)	$\gg 10^b$
MDH-2 IC_{50} (UV endpoint)	$\gg 10^b$

^a See Supplementary data for experimental details associated with each assessment. All biochemical and SPR assay results are reported as the arithmetic mean of 2 separate runs ($n = 2$).

^b No inhibition of either MDH-1 or MDH-2 was observed at the highest concentration tested (10 μM). MDH = malate dehydrogenase.

suggested that optimal binding of **5** to LDHA required prior association of the NADH co-factor in a manner that might parallel events occurring during the catalytic conversion of pyruvate to lactate.¹⁸

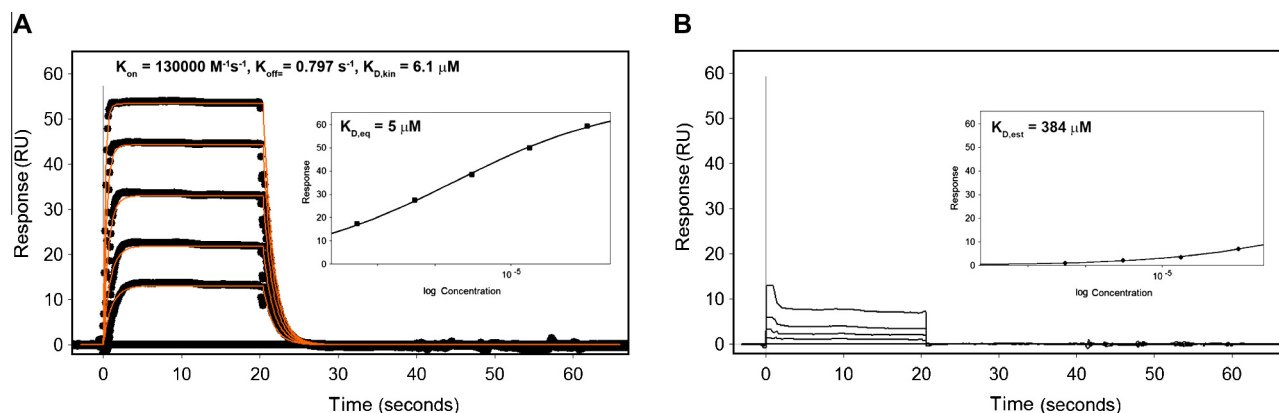


Figure 3. SPR data depicting the binding of compound **5** to LDHA in the presence (A) and absence (B) of NADH. The K_D 's determined from fitting the kinetics or the equilibrium dose response (inset) are reported in panel A. In panel B, the K_D was estimated relative to a control using methods described in the [Supplementary data](#). In both panels, the top concentration is 25 μM with injections related by a twofold dilution series. See [Supplementary data](#) for additional experimental details.

Saturation transfer difference (STD) NMR experiments showed a strong NADH-related signal which disappeared upon addition of compound **5** to the NADH/LDHA mixture (Fig. 4).¹⁶ This behavior is consistent with the simultaneous binding of **5** and NADH to LDHA in a manner which inhibits the fast on-off binding exchange of the co-factor.¹⁹ A similar result was obtained when oxamate was added to the STD experiment (Fig. 4) suggesting that this entity did not interfere with the binding of **5** to LDHA. Consistent with these observations, the co-crystal structure of a related 2-thio-6-oxo-1,6-dihydropyrimidine with LDHA suggested that the inhibitor, NADH, and oxamate could simultaneously bind to the protein (see below).

In addition to the detailed characterization activities described above, we also examined the ability of compound **5** to inhibit the biochemical activity of other dehydrogenase enzymes. As shown in Table 1, the molecule inhibited the closely related LDHB isoform

with an IC_{50} value nearly identical to that observed for LDHA. This result was not entirely surprising given the close structural homology between these two enzymes.²⁰ Encouragingly, compound **5** displayed only weak inhibition of two other structurally-related²¹ dehydrogenases (malate dehydrogenase 1 and malate dehydrogenase 2, Table 1) suggesting that the molecule would not indiscriminately inhibit this class of enzymes.¹⁶

Intrigued by the potency and specificity of **5**, we initiated medicinal chemistry activities aimed at improving the compound's LDHA inhibition properties. As shown in Table 2, methylation of the sulfonamide functional group contained in **5** resulted in significant loss of anti-LDHA activity (compare **6** with **5**). Similarly, replacement of the *para*- H_2NSO_2 -aniline moiety present in **5** with other substituted anilines reduced LDHA inhibition potency to varying degrees (compounds **7–18**, Table 2). These potency

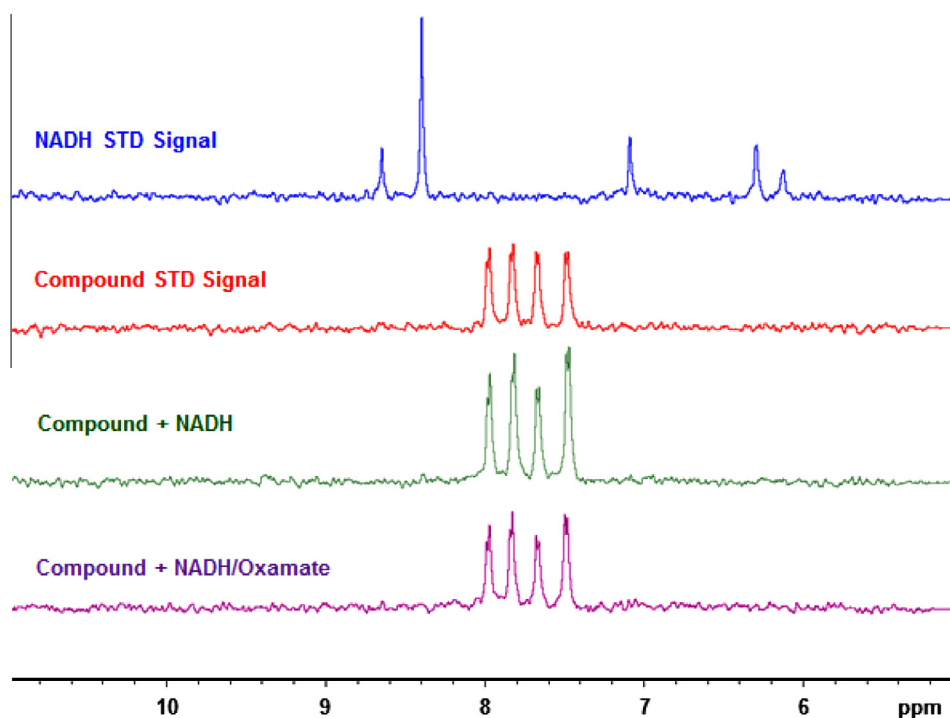
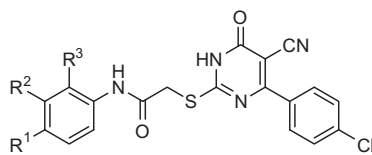


Figure 4. Saturation transfer difference NMR experiments performed with LDHA (3 μM), NADH (500 μM ; blue trace), compound **5** (500 μM ; red trace), compound **5** and NADH (500 and 500 μM , respectively; green trace) and compound **5** with NADH and oxamate (500, 500 μM and 2.5 mM, respectively; magenta trace). See [Supplementary data](#) for additional experimental details.

Table 2
Structure–activity relationships of 6-oxo-1,6-dihydropyrimidine-containing compounds



Compd	R ¹	R ²	R ³	LDHA IC ₅₀ ^a (μM)	LDHA K _D ^b (μM)	LDHB IC ₅₀ ^c (μM)
5	H ₂ NS(O ₂)–	H	H	8.8	6.1	11.1
6	MeNHS(O ₂)–	H	H	>100	532	>100
7	Cl	H	H	55.7	570	>100
8	ⁱ Pr	H	H	22.6	552	98
9	H	H	Me	>100	1011	ND
10	H	H	OMe	>100	1105	ND
11	H	H	Et	>100	1215	ND
12	H	Cl	H	55.8	386	>100
13	H	Cl	Me	50.2	462	>100
14	H	Me	Me	>100	1055	ND
15	F	Cl	H	46.8	314	>100
16	Me	Cl	H	27.6	466	93
17	MeO	Cl	H	26.5	640	>100
18	Me	Me	H	38.6	552	>100

See [supplementary data](#) for experimental details associated with each assessment. All biochemical and SPR assay results are reported as the arithmetic mean of 2 separate runs ($n = 2$). ND = not determined.

^a LDHA biochemical inhibition.

^b LDHA dissociation constant as determined by surface plasmon resonance.

^c LDHB biochemical inhibition.

reductions were subsequently explained by the crystallographic observation of several critical protein–ligand interactions between the *para*-H₂NSO₂ moiety of an inhibitor related to **5** and the LDHA protein (see below). LDHB inhibition activities for compounds **6**–**18** were generally weak and were typically two- to threefold less potent than the corresponding LDHA values. Importantly, the LDHA K_D's determined by SPR for the compounds in [Table 1](#) in the presence of NADH paralleled the IC₅₀ measurements with less potent biochemical inhibitors exhibiting weaker K_D values. This observation reinforced the belief that compound **5** and related molecules derived their LDHA inhibition activities primarily through specific interactions with the protein.

Having determined that the *para*-H₂NSO₂-aniline moiety present in **5** was critical for anti-LDHA potency, we next explored modifying other portions of the inhibitor's structure. As shown in [Table 3](#), substitution of the *para*-Cl-Ph moiety contained in **5** with a simple phenyl group afforded slightly diminished LDHA inhibition activity (compare **19** with **5**). However, similar replacement with a *meta*-MeO-Ph group resulted in more dramatic loss of inhibitory potency (compound **20**, [Table 3](#)). The described SAR is consistent with subsequent crystallographic observations indicating the lack of appropriate space to accommodate a relatively large *meta*-Ph substituent in this portion of the 6-oxo-1,6-dihydropyrimidine moiety (see below). Substitution of the aliphatic methylene present in **5** with a methyl group improved LDHA inhibition activity by more than 10-fold (compare **21** with **5**, [Table 3](#)). This enhancement was largely retained when additional small substituents were added to the *para*-Cl-Ph moiety contained in **21** (compounds **22** and **23**). Interestingly, removal of the nitrile group attached to the 2-thio-6-oxo-1,6-dihydropyrimidine ring system resulted in drastic potency loss (compound **24**, [Fig. 5](#); also removes *para*-Cl substituent relative to **21**). The nitrile present in the related inhibitor **22** was subsequently shown by crystallography to make a hydrogen bond with a structural water molecule (see below) and removal of this protein–ligand interaction may explain the observed loss in activity. However, given the magnitude of the potency reduction, it is possible that the nitrile also performs other functions which favorably impact LDHA inhibition (e.g., influenc-

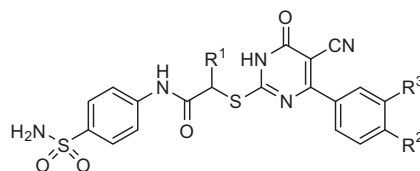
ing the 6-oxo-1,6-dihydropyrimidine tautomer distribution and/or pK_a).²² Replacement of the *para*-Cl-Ph moiety present in **21** with a hydrogen atom afforded a less potent inhibitor (compound **25**, [Fig. 5](#)), although the observed activity reductions were not as pronounced as those resulting from nitrile removal. Substituting the methyl group present in **21** with an ethyl moiety afforded a molecule with similar LDHA inhibition properties (compound **26**, [Table 3](#)). Incorporation of the same ethyl fragment into a compound containing a *meta*-MeO-Ph 6-oxo-1,6-dihydropyrimidine substituent improved LDHA inhibition activity approximately fivefold (compare compounds **27** and **20**, [Table 3](#)). A rationalization for the potency improvements obtained by substituting the aliphatic methylene present in **5** and/or **20** with methyl or ethyl groups is provided in the crystallography discussion below.

As was observed for the compounds depicted in [Table 2](#), the LDHB activities of the inhibitors described in [Table 3](#) were typically several fold weaker than the corresponding LDHA values. Similarly, the LDHA K_D's determined by SPR for the molecules in [Table 3](#) paralleled their LDHA biochemical IC₅₀ potencies with the most active inhibitors exhibiting the strongest LDHA biophysical associations (e.g., compounds **21**–**23**, and **26**). The majority of these compounds were also stable in the presence of human liver microsomes and afforded extrapolated human clearance values in the low to moderate range. In addition, the aqueous solubilities of the most potent inhibitors were measured and were determined to be acceptable ([Table 3](#), compounds **21**–**23**, and **26**).

We also assessed the ability of compounds **21**–**23** to inhibit the production of lactate in HCC1954 cells.¹⁶ Unfortunately, none of the molecules displayed activity in this assay when tested up to the 50 μM concentration level. The reasons for this lack of cell-based activity are currently not known with certainty but may include: (1) insufficient biochemical potency, (2) poor cell permeability, and/or (3) high protein binding.²³ Additional experiments are on-going to clarify which, if any, of these potential liabilities is responsible for the poor cell-based activity exhibited by the described 6-oxo-1,6-dihydropyrimidine-containing compounds.

To aid in the future optimization of this inhibitor series, a crystal structure of compound **22** in complex with LDHA was obtained

Table 3
Structure–activity relationships of 6-oxo-1,6-dihydropyrimidine-containing compounds



Compd	R ¹	R ²	R ³	LDHA IC ₅₀ ^a (μM)	LDHA K _D ^b (μM)	LDHB IC ₅₀ ^c (μM)	HLM Cl ^d (mL/min/kg)	Solubility ^e (μM)
5	H	Cl	H	8.8	6.1	11.1	5.3	ND
19	H	H	H	12.1	15.4	42.8	ND	ND
20	H	H	OMe	42.4	38.4	56.4	ND	ND
21^f	Me	Cl	H	0.48	2.2	3.0	2.6	58
22^f	Me	Cl	Cl	0.75	5.1	3.7	2.6	30
23^f	Me	Cl	F	0.71	2.9	2.3	3.4	64
26^f	Et	Cl	H	0.65	3.0	2.4	2.8	136
27^f	Et	H	OMe	7.4	8.9	7.7	6.9	ND

See Supplementary data for experimental details associated with each assessment. All biochemical and SPR assay results are reported as the arithmetic mean of 2 separate runs ($n = 2$). HLM and solubility data are $n = 1$. ND = not determined.

^a LDHA biochemical inhibition.

^b LDHA dissociation constant as determined by surface plasmon resonance.

^c LDHB biochemical inhibition.

^d In vivo clearance value extrapolated from in vitro human liver microsome experiment (key: stable = <6.2; labile = >15).

^e Aqueous solubility (estimated from high-throughput assay).

^f Racemic.

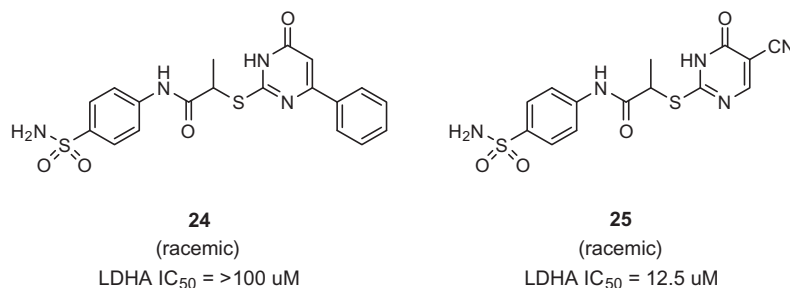


Figure 5.

(1.90 Å resolution).²⁴ As shown in Figure 6a, the molecule bound to the protein near several conserved residues involved in the catalytic processing of LDH substrates (Arg-168, His-192 and Asp-165).²⁵ Interestingly, the inhibitor did not form any direct interactions with these residues but was instead found contacting an adjacent region of the protein known to undergo significant conformational changes during the enzyme's catalytic cycle (key mobile residue = Arg-105).⁵ The presence of compound **22** resulted in a relatively 'open' conformation of this region in which a fourth conserved residue required for enzyme catalysis (Arg-105) was positioned well-removed from the substrate binding site. The ~7 Å distance between **22** and the Arg-168 and His-192 catalytic residues suggested that small LDH substrate mimetics could simultaneously occupy the enzyme's active site. This observation is consistent with the STD NMR data described above indicating that a related inhibitor (compound **5**) and oxamate (a small substrate mimetic) do not interfere with each other's binding to LDHA.

The NADH co-factor was observed in the crystal structure and bound to LDHA adjacent to compound **22** in a location and orientation similar to those previously described in the literature.²⁶ As shown in Figures 6b and 6d, the carbonyl of the inhibitor 6-oxo-1,6-dihydropyrimidine moiety²⁷ formed a hydrogen bond with the NADH 2'-OH group. In addition, the nitrile present in **22** was located within H-bond distance of both the LDHA Gln-99 backbone amide NH group and a crystallographic water molecule. The latter

entity formed hydrogen bonds with the NADH 3'-OH group and the backbone carbonyl of the LDHA Ala-97 residue. These interactions between **22** and NADH are consistent with the SPR data described earlier in this work which indicated that the compound exhibits much greater affinity for the LDHA protein in the presence of the co-factor.

Although inhibitor **22** was prepared in racemic form, only one enantiomer (the *R*-Me isomer) was observed in the co-crystal structure with LDHA. The methyl group present in **22** formed favorable hydrophobic contacts with the LDHA Tyr-238 side chain, suggesting why addition of aliphatic substituents to the methylene moiety present in the original screening hit (**5**) improved LDHA inhibition activity (Fig. 6b). Such substituents may also help enforce the twisted conformation of the bound inhibitor observed in the **22**-LDHA co-crystal structure.²⁸ In addition, hydrogen bonds were observed between the aniline-amide NH of the inhibitor and the side chain of LDHA residue Asp-194 as well as between the aniline-amide carbonyl moiety and a crystallographic water molecule (Figs. 6b and 6d). These interactions presumably contribute to the compound's anti-LDHA activity.

As expected based on the SAR described in the preceding section, the *para*-H₂NSO₂-aniline substituent contained in **22** formed numerous favorable interactions with the LDHA protein. These associations include: (1) a hydrogen bond between the sulfonamide NH₂ moiety and the side chain of LDHA residue Asp-140,

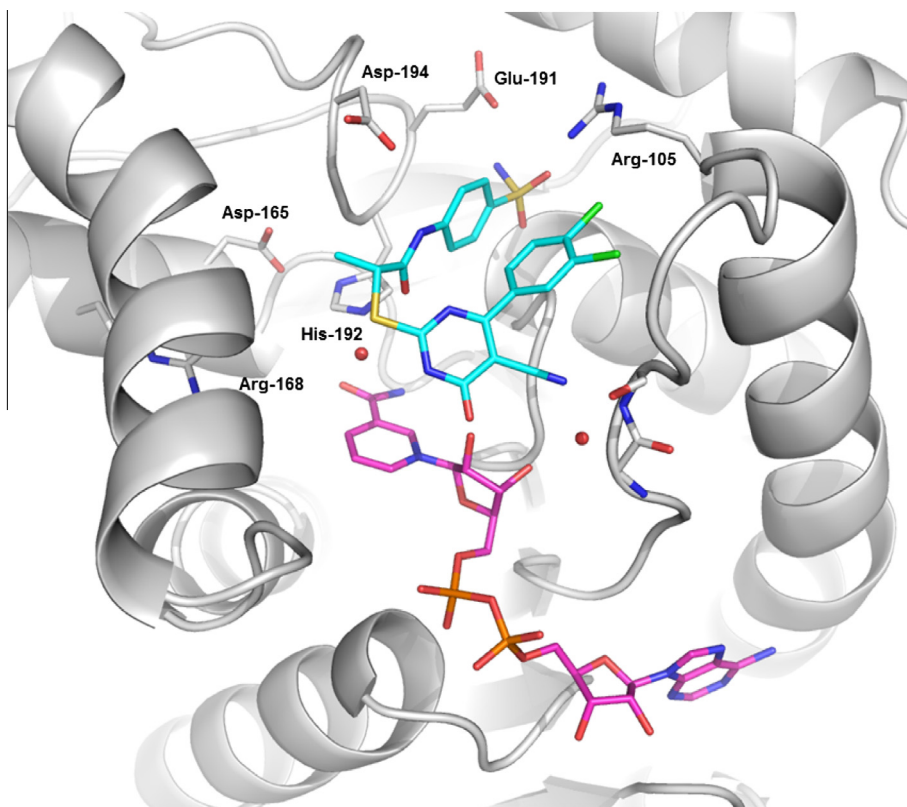


Figure 6a. Co-crystal structure of inhibitor **22** (cyan) in complex with LDHA (grey). NADH is also present and is depicted in pink. Key structural waters are also shown (red spheres). Hydrogen bonds are not depicted in this figure. The resolution of the structure is 1.90 Å.

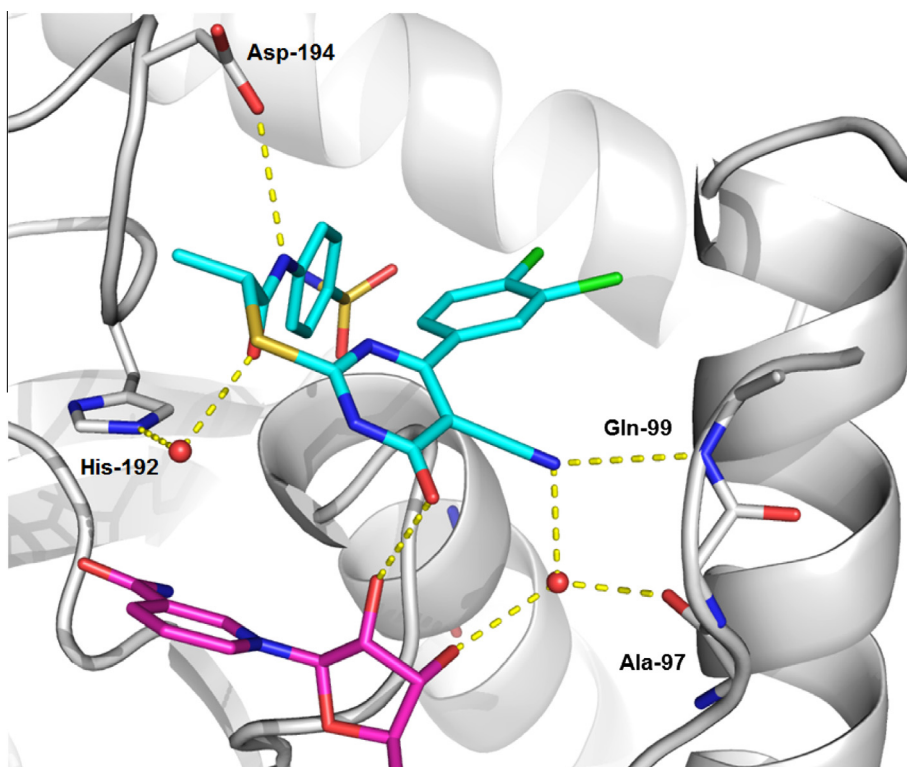


Figure 6b. Alternate view of co-crystal structure of inhibitor **22** (cyan) in complex with LDHA (grey). NADH is also present and is depicted in pink. Key structural waters are also shown (red spheres). Hydrogen bonds are depicted as dashed yellow lines.

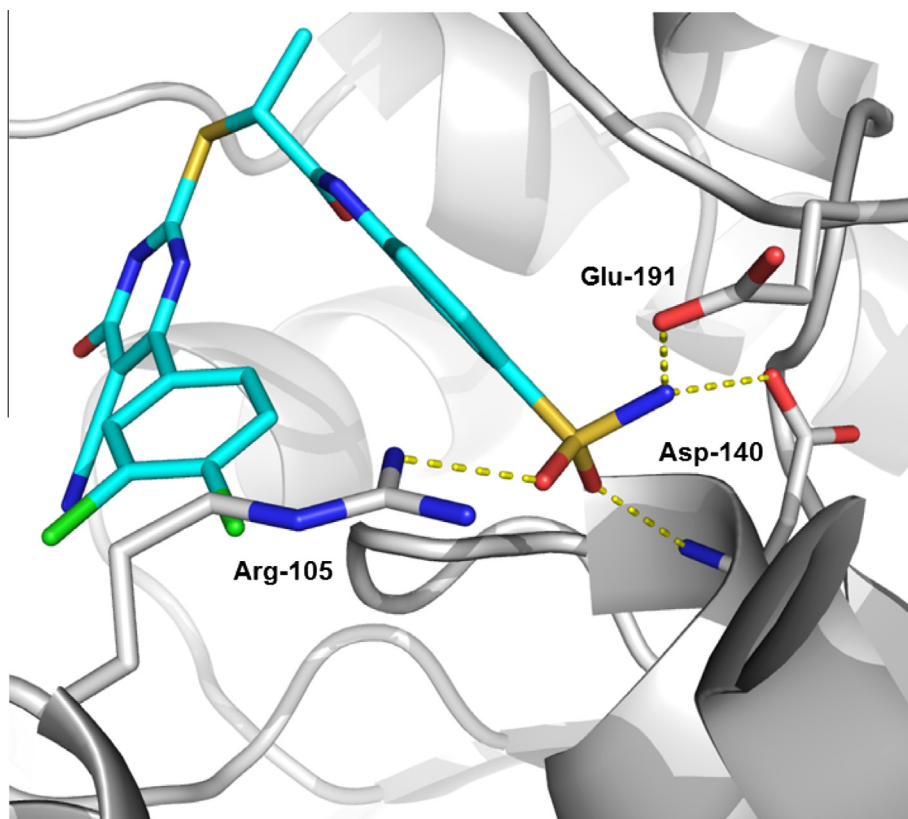


Figure 6c. Alternate view of co-crystal structure of inhibitor **22** (cyan) in complex with LDHA (grey). Hydrogen bonds are depicted as dashed yellow lines.

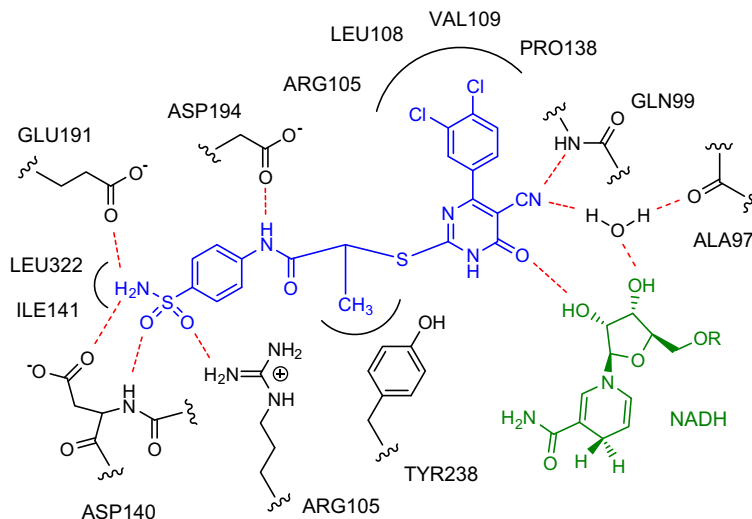
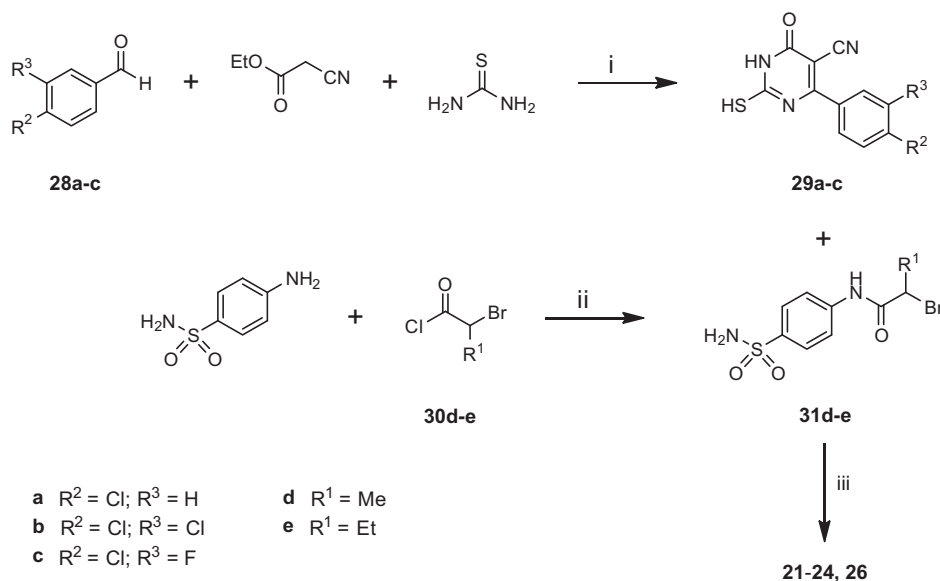


Figure 6d. Depiction of key protein–ligand interactions observed in **22**-LDHA co-crystal structure. Hydrogen bonds are depicted as dashed lines. An H-bond interaction between a water molecule and the amide carbonyl of **22** is omitted for clarity.

(2) another hydrogen bond between the sulfonamide NH_2 and the Glu-191 side chain, (3) a hydrogen bond between a sulfonamide O-atom and the backbone NH of Asp-140, and (4) a hydrogen bond between the other sulfonamide O-atom and the side chain of Arg-105 (Figs. 6c and 6d). These interactions explain the loss of inhibition potency described earlier in this work that resulted either from methylation of the *para*- H_2NSO_2 -moiety or its removal from the inhibitor structure. In addition, the sulfonamide group was observed in close proximity to the side chains of LDHA residues Ile-141 and Leu-322 suggesting that accommodation of elongated (i.e., alkylated) analogs would be difficult.

The 3,4-di-Cl-Ph moiety present in **22** was observed crystallographically to reside in a primarily hydrophobic cleft formed by the side chains of LDHA residues Arg-105, Leu-108, Val-109, and Pro-138 (Figs. 6c and 6d). The 3-Cl substituent on the phenyl ring was oriented away from the ligand's *para*- H_2NSO_2 -aniline group, presumably to avoid an intramolecular steric clash that would disrupt the observed binding conformation of the inhibitor. The 3-Cl substituent made close contacts with the surrounding LDHA residues, and this binding mode was consistent with the observation that incorporation of a larger OMe group at the *meta*-position of the inhibitor Ph ring was detrimental to anti-LDHA activity (see



Scheme 1. Synthesis of 2-thio-6-oxo-1,6-dihydropyrimidine-containing compounds. Reagents and conditions: (i) K_2CO_3 , ethanol, reflux, 1 h or piperidine, ethanol, 5 h; (ii) K_2CO_3 , THF, reflux, 1 h; and (iii) K_2CO_3 , ethanol, reflux, 1–24 h.

above). Collectively, the **22**-LDHA co-crystal structure illustrates that the inhibitor makes numerous hydrogen bonds with the LDHA protein, the NADH co-factor, and crystallographic water molecules along with several favorable hydrophobic protein–ligand interactions. This structural information can be utilized to design new 2-thio-6-oxo-1,6-dihydropyrimidine-containing LDHA inhibitors that seek to improve the potency of the molecules detailed in this work.

The described inhibitors were either purchased from eMolecules (**5**, **7**–**20**, **25**, **27**) or were synthesized as depicted in Scheme 1 (**6**, **21**–**24**, **26**). Synthesis commenced with the condensation of various benzaldehydes (**28a**–**c**) with ethyl 2-cyanoacetate and thiourea to give the corresponding 2-thio-6-oxo-1,6-dihydropyrimidines (**29a**–**c**).²⁹ Separately, bromides **31d**–**e** were prepared via coupling of 4-aminobenzenesulfonamide with acid chlorides **30d** (commercially available) and **30e** (synthesized as described in the literature³⁰). Appropriate condensation of the 2-thio-6-oxo-1,6-dihydropyrimidines **29** with bromides **31** subsequently afforded the desired LDHA inhibitors **21**–**24** and **26** in good yields. Compound **6** was prepared in an analogous manner with the required 4-amino-*N*-methylbenzenesulfonamide being synthesized as described in the literature.³¹

In summary, a novel class of 2-thio-6-oxo-1,6-dihydropyrimidine-containing LDHA inhibitors was identified using a high throughput screening approach. The crystal structure of a representative compound in complex with the protein indicated that these inhibitors bound in the LDHA active site but did not make direct interactions with the majority of enzyme residues involved in substrate catalysis. Structural modification of the initial high throughput screening hit afforded >10-fold improvements in biochemical potency, but none of the molecules studied were active in cell culture experiments. Additional efforts to obtain potent, cell-active LDHA inhibitors will be reported in due course.

Acknowledgments

We thank Drs. Krista Bowman and Jiansheng Wu and their respective Genentech research groups for performing many associated protein expression and purification activities. We also thank Dr. Peter Jackson for many helpful discussions regarding LDHA. In addition, we thank Crystallographic Consulting, LLC for

diffraction data collection. The Advanced Light Source is supported by the Director, Office of Science, Office of Basic Energy Sciences, of the U.S. Department of Energy under Contract No. DE-AC02-05CH11231.

Supplementary data

Supplementary data associated with this article can be found, in the online version, at <http://dx.doi.org/10.1016/j.bmcl.2013.04.001>.

References and notes

- (a) Ward, P. S.; Thompson, C. B. *Cancer Cell* **2012**, *21*, 297; (b) Vander Heiden, M. G. *Nat. Rev. Drug Disc.* **2011**, *10*, 671; (c) Zhao, Y.; Liu, H.; Riker, A. I.; Fodstad, O.; Ledoux, S. P.; Wilson, G. L.; Tan, M. *Front. Biosci.* **2011**, *16*, 1844; (d) Kaelin, W. G., Jr.; Thompson, C. B. *Nature* **2010**, *465*, 562; (e) Tennant, D. A.; Durán, R. V.; Gottlieb, E. *Nat. Rev. Cancer* **2010**, *10*, 267.
- (a) Vander Heiden, M. G.; Cantley, L. C.; Thompson, C. B. *Science* **2009**, *324*, 1029; (b) Hsu, P. P.; Sabatini, D. M. *Cell* **2008**, *134*, 703.
- (a) Warburg, O. *Science* **1956**, *123*, 309; (b) Bensinger, S. J.; Christofk, H. R. *Semin. Cell Dev. Biol.* **2012**, *23*, 352; (c) Koppenol, W. H.; Bounds, P. L.; Dang, C. V. *Nat. Rev. Cancer* **2011**, *11*, 325.
- (a) Hamanaka, R. B.; Chandel, N. S. *J. Exp. Med.* **2012**, *209*, 211; (b) Jones, N. P.; Schulze, A. *Drug Discovery Today* **2011**, *17*, 232; (c) Pelicano, H.; Martin, D. S.; Xu, R.-H.; Huang, P. *Oncogene* **2006**, *25*, 4633.
- Granchi, C.; Bertini, S.; Macchia, M.; Minutolo, F. *Curr. Med. Chem.* **2010**, *17*, 672.
- For a detailed description of glycolysis, see: Salway, J. G. *Metabolism at a Glance*, 3rd ed.; Blackwell Publishing: Malden, 2004. pp 10–25.
- LDHA and LDHB are each homotetramers comprised of M and H subunits, respectively. LDH heterotetramers containing both M and H subunits are also known. For more information, see Ref. 5.
- (a) Kolev, Y.; Uetake, H.; Takagi, Y.; Sugihara, K. *Ann. Surg. Oncol.* **2008**, *15*, 2336; (b) Koukourakis, M. I.; Giatromanolaki, A.; Sivridis, E.; Gatter, K. C.; Harris, A. L. *J. Clin. Oncol.* **2006**, *24*, 4301; (c) Koukourakis, M. I.; Giatromanolaki, A.; Sivridis, E.; Bougioukas, G.; Didiilis, V.; Gatter, K. C.; Harris, A. L. *Br. J. Cancer* **2003**, *89*, 877.
- (a) Seth, P.; Grant, A.; Tang, J.; Vinogradov, E.; Wang, X.; Lenkinski, R.; Sukhatme, V. P. *Neoplasia* **2011**, *13*, 60; (b) Qing, G.; Skuli, N.; Mayes, P. A.; Pawel, B.; Martinez, D.; Maris, J. M.; Simon, M. C. *Cancer Res.* **2010**, *70*, 10351; (c) Fantin, V. R.; St-Pierre, J.; Leder, P. *Cancer Cell* **2006**, *9*, 425.
- Le, A.; Cooper, C. R.; Gouw, A. M.; Dinavahi, R.; Maitra, A.; Deck, L. M.; Royer, R. E.; Vander Jagt, D. L.; Semenza, G. L.; Dang, C. V. *Proc. Natl. Acad. Sci.* **2010**, *107*, 2037.
- Ward, R. A.; Brassington, C.; Breeze, A. L.; Caputo, A.; Critchlow, S.; Davies, G.; Goodwin, L.; Hassall, G.; Greenwood, R.; Holdgate, G. A.; Mrosek, M.; Norman, R. A.; Pearson, S.; Tart, J.; Tucker, J. A.; Vogtherr, M.; Whittaker, D.; Wingfield, J.; Winter, J.; Hudson, K. J. *J. Med. Chem.* **2012**, *55*, 3285.

12. (a) Kanno, T.; Sudo, K.; Maekawa, M.; Nishimura, Y.; Ukita, M.; Fukutake, K. *Clin. Chim. Acta* **1988**, *173*, 89; (b) Kanno, T.; Sudo, K.; Takeuchi, I.; Kanda, S.; Honda, N.; Nishimura, Y.; Oyama, K. *Clin. Chim. Acta* **1980**, *108*, 267.
13. Granchi, C.; Roy, S.; Giacomelli, C.; Macchia, M.; Tuccinardi, T.; Martinelli, A.; Lanza, M.; Betti, L.; Giannaccini, G.; Lucacchini, A.; Funel, N.; León, L. G.; Giovannetti, E.; Peters, G. J.; Palchadhuri, R.; Calvaresi, E. C.; Hergenrother, P. J.; Minutolo, F. *J. Med. Chem.* **2011**, *54*, 1599.
14. (a) For additional examples of LDH inhibitors, see: Kohlmann, A.; Zech, S. G.; Li, F.; Zhou, T.; Squillace, R. M.; Commodore, L.; Greenfield, M. T.; Lu, X.; Miller, D. P.; Huang, W.-S.; Qi, J.; Thomas, R. M.; Wang, Y.; Zhang, S.; Dodd, R.; Liu, S.; Xu, R.; Xu, Y.; Miret, J. J.; Rivera, V.; Clackson, T.; Shakespeare, W. C.; Zhu, X.; Dalgarno, D. C. *J. Med. Chem.* <http://dx.doi.org/10.1021/jm3014844>; (b) Chai, D.; Colon, M.; Dodson, C.; Duffy, K. J.; Shaw, A. N. *WO* 2012/061557; In addition, inhibitors of *Plasmodium falciparum* LDH with potential for use as anti-malarials have been described: (c) Choi, S.-R.; Pradham, A.; Hammond, N. L.; Chittiboyina, A. G.; Tekwani, B. L.; Avery, M. A. *J. Med. Chem.* **2007**, *50*, 3841; (d) Choi, S.-R.; Beeler, A. B.; Pradham, A.; Watkins, E. B.; Rimoldi, J. M.; Tekwani, B.; Avery, M. A. *J. Comb. Chem.* **2007**, *9*, 292; (e) Cameron, A.; Read, J.; Tranter, R.; Winter, V. J.; Sessions, R. B.; Brady, R. L.; Vivas, L.; Easton, A.; Kendrick, H.; Croft, S. L.; Barros, D.; Lavandera, J. L.; Martin, J. J.; Risco, F.; García-Ochoa, S.; Gamo, F. J.; Sanz, L.; Leon, L.; Ruiz, J. R.; Gabarró, R.; Mallo, A.; Gómez de la Heras, F. *J. Biol. Chem.* **2004**, *279*, 31429.
15. VanderPorten, E.; Frick, L.; Turincio, R.; Thana, P.; LaMarr, W.; Liu, Y. *Anal. Biochem.*, submitted for publication.
16. See Supplementary data for details regarding enzyme, SPR, NMR, and cell culture assay methods.
17. No attempts were made to identify which, if any, dihydropyrimidine tautomers predominated in organic and/or aqueous solutions. All new compounds described in this work are arbitrarily drawn and described as 6-oxo-1,6-dihydropyrimidines.
18. Binding of NADH to LDHA precedes binding of the pyruvate in the accepted LDHA catalytic mechanism. See Ref. 5 for additional details.
19. The STD NMR results are also consistent with complete displacement of NADH from the LDHA protein by the binding of compound **5**.
20. Read, J. A.; Winter, V. J.; Eszes, C. M.; Sessions, R. B.; Brady, R. L. *Proteins* **2001**, *43*, 175.
21. Human LDHA and human MDH-2 protein sequences share 20% similarity. X-ray structures of their protomers can be superimposed using 173 pairs of Ca atoms with an rms deviation of 1.7 Å. Ca atoms within 5 Å of bound NADH can be superimposed with an rms deviation of 0.7 Å.
22. The pK_a of compound **26** was measured and was determined to be relatively acidic (3.94).
23. Compounds **21–23** bind strongly to human and animal plasma proteins (free unbound fractions <1% in all cases examined). The apparent apical to basolateral permeability of compound **21** determined using Madin–Darby canine kidney (MDCK) cell monolayers was relatively low ($P_{app, A-B} = 0.30 \times 10^{-6}$ cm/s) with minimal efflux noted ($A-B/B-A = 0.69$).
24. See the Supplementary data for experimental details associated with the described co-crystal structure. All crystallographic descriptions are based on analysis of the ligand chain 'X'/protein chain 'C' LDHA protomer. Two other LDHA protomers containing bound ligand were also observed in the tetramer asymmetric unit. The protein–ligand interactions noted in these other protomers were similar to those described for the ligand chain 'X'/protein chain 'C' complex, although some subtle differences were apparent. See deposited PDB file for additional structural details: code = 4JNK.
25. The LDH residue numbering scheme used herein follows the convention of PDB entries 1110 and 4AJJ which does not account for the initiating methionine in the gene sequence reflected in UniProt entry P00338. This numbering scheme differs by one residue from that described elsewhere: Chung, F. Z.; Tsujibo, H.; Bhattacharyya, U.; Sharief, F. S.; Li, S. S. *Biochem. J.* **1985**, *231*, 537.
26. For other examples of LDH crystal structures containing NADH, see Ref. 20 and Chaikvad, A.; Fairweather, V.; Connors, R.; Joseph-Horne, T.; Turgut-Balik, D.; Brady, R. L. *Biochemistry* **2005**, *44*, 16221.
27. The resolution of the LDHA-**22** co-crystal does not allow for precise determination of the inhibitor tautomer that is bound to the protein. The compound is arbitrarily described as a 6-oxo-1,6-dihydropyrimidine in discussion of the co-crystal structure.
28. To assess the effect of the methyl group on inhibitor conformation, a dihedral angle scan of the C–S bond was performed on the bound conformation of compound **22** and its des-methyl counterpart using MacroModel (Schrodinger Maestro v9.2) with OPLS-2005 force field and default parameters. The results show that, although the methyl group does not alter the global minima, there is a competing local minimum if the methyl is absent, thus creating an entropic penalty toward binding for the des-methyl molecule. See the Supplementary data for additional details.
29. (a) Chen, W.; Huang, Y.-J.; Gundala, S. R.; Yang, H.; Li, M.; Tai, P. C.; Wang, B. *Bioorg. Med. Chem.* **2010**, *18*, 1617; (b) Kambe, S.; Saito, K.; Kishi, H. *Synthesis* **1979**, 287.
30. Boschi, F.; Camps, P.; Comes-Franchini, M.; Muñoz-Torrero, D.; Ricci, A.; Sánchez, L. *Tetrahedron: Asymmetry* **2005**, *16*, 3739.
31. Khanna, I. K.; Weier, R. M.; Yu, Y.; Collins, P. W.; Miyashiro, J. M.; Koboldt, C. M.; Veenhuizen, A. W.; Currie, J. L.; Seibert, K.; Isakson, P. C. *J. Med. Chem.* **1997**, *40*, 1619.